On-Line Tracking of Inertia Constants Using Ambient Measurements

Stelios C. Dimoulias, Eleftherios O. Kontis, and Grigoris K. Papagiannis

***Abstract*—In this paper, a new method for on-line inertia estimation is developed. The proposed method is based on the sliding window concept and uses ambient responses, i.e., responses obtained during the normal operation of the power system, to identify inertia constants of generation devices. The effectiveness of the developed method is evaluated by means of simulations on two benchmark power system models, namely the IEEE 9-Bus Test System and the IEEE 39-Bus Test System. The conducted analysis reveals that the proposed method can accurately identify inertia constants of conventional synchronous generators (SGs), converter-interfaced units operated as virtual SGs, and virtual power plants. The performance of the proposed method is also evaluated under noisy conditions, by performing Monte Carlo simulations. Finally, comparisons with conventional methods are performed, demonstrating the superior performance of the developed method.**

***Index Terms*—Ambient data, frequency stability, inertia estimation, power system dynamics, system identification.**

I. Introduction

The worldwide drive for reduction of carbon emissions has led to the gradual decommissioning of conventional synchronous generators (SGs), driven by fossil fuels, and the widespread introduction of inverter-based renewable energy sources (RESs) [1]. Nevertheless, this shift towards non-synchronous generation is expected to have a significant impact on the operation and control of power systems [2].

The most important challenge, introduced due to the increased penetration of inverter-based generation, is the reduction of the overall rotational system inertia [3], [4], which is traditionally provided by the conventional SGs. The natural inertial response contributes to the mitigation of frequency excursions during system disturbances, while also limiting the rate of change of frequency (RoCoF) [4]. Therefore, the reduction of natural inertia leads to lower frequency nadirs and higher RoCoF values, jeopardizing the overall grid stability [2]. Additionally, the intermittent nature of RESs renders inertia levels variable during the day, thus further complicating the frequency control of modern power systems [2].

To overcome these challenges, inertial control functionalities are embedded nowadays to RESs [5], [6]. System operators can remotely adjust control settings of these sources to modify their inertia constants, thus ensuring improved frequency responses. These new control functionalities will allow large-scale RESs to participate in ancillary service (AS) markets, to trade inertia products [7]. Additionally, aggregator entities (or distribution system operators) can create portfolios of small-scale RESs, connected to the distribution grid, so as to participate in future energy markets, by providing inertia as an AS to the transmission system (TS) [8].

In this context, TS operators (TSOs) shall be able to monitor in real-time the inertia contribution of each generation unit, in order to ensure the fair remuneration of all market participants. Additionally, TSOs shall be able to assess, using real-time measurements, the overall inertia levels of their grids. In case of low inertia levels, remedial actions, such as re-dispatching of controllable RESs and deployment of synchronous condensers, shall be activated to ensure grid stability [9].

Therefore, during the last years, several efforts have been dedicated to the development of inertia estimation techniques [10], [11]. For instance, in [12], a closed-loop identification method is developed to estimate, in real-time, inertia time constants of SGs. However, this approach requires the injection of well-designed probing signals, which complicates its implementation [1]. Non-intrusive methods have also been proposed [13]–[15]. These methods are based on the development of low-order transfer function models, that describe the relationship between active power changes and the resulting frequency deviations. Non-intrusive methods utilize either ringdown (transient) responses or ambient data, i.e., responses that reflect the dynamic behavior of the power system under the random variations of load and RESs. The former approach requires data from large disturbances to perform satisfactorily, i.e., to provide accurate inertia estimates. Therefore, it is not suitable for on-line tracking of inertia constants. The latter approach uses data from normal operating conditions, thus facilitating the development of on-line estimation techniques.

In non-intrusive methods, parameters of the required input-output transfer functions are estimated using optimization methods or system identification techniques [11]. Estimates of inertia constants are derived on a second stage, by processing the parameters of the developed transfer functions. Several post-processing methods have been developed to derive inertia constants from the parameters of the identified transfer functions. For instance, in [15], the developed transfer functions are reduced to first order counterparts, by eliminating insignificant states. The resulted first order transfer functions have the general form of the swing equation, thus allowing for the determination of inertia constants. Nevertheless, order reduction may introduce significant errors on inertia estimates. This is especially true under noisy conditions [16]. To avoid order reduction, in [14] and [17], the impulse response of the identified transfer functions is used to determine inertia constants, while in [13] and [18] the initial slope of the unit

Stelios C. Dimoulias, E. O. Kontis, and Grigoris K. Papagiannis are with the Power Systems Laboratory, School of Electrical and Computer Engineering, Aristotle University of Thessaloniki, Thessaloniki, Greece, GR 54124, (e-mail: steliosd@ece.auth.gr; ekontis@ece.auth.gr; gpapagia@ece.auth.gr).

step response of the derived transfer functions is utilized.

Nevertheless, existing non-intrusive methods, that use ambient data to estimate inertia constants, present certain shortcomings and limitations. Indeed, these methods generally require long observation periods, in the order of hundreds of seconds, to perform satisfactorily [13], [14]. However, as the length of the analysis window increases, the computational burden increases as well, hindering the real-time update of inertia estimates. Moreover, the accuracy of these methods is highly affected by the approximation order, i.e., the order of the developed transfer function. To handle this issue either iterative procedures shall be adopted [13] or transfer functions of various orders shall be developed [14]. Nevertheless, both approaches increase the computational complexity. Additionally, in these approaches, poorly identified models may arise, resulting in unrealistic inertia estimates [11]. Finally, due to data quality issues, the identification procedure may lead to unstable transfer functions [16]. In these cases, the identified models cannot be used for inertia estimation.

To overcome these issues, in this paper, a new method for the on-line tracking of inertia constants is developed. The proposed method is based on the sliding window (SW) concept and uses ambient data, i.e., normal operation responses, that are always available to system operators. More specifically, ambient responses of frequency and active power are recorded at the terminals of generation devices. Using these responses, low-order transfer function models are developed by means of the Auto-Regressive Moving Average eXogenous (ARMAX) method. The derived models are further processed and inertia constants are extracted using an automated procedure. The accuracy of the proposed method is evaluated by means of simulations on two benchmark power systems, namely the IEEE 9-Bus Test System and the IEEE 39-Bus Test System. The advantages of the proposed method are summarized in the following aspects:

- *Computational Complexity*. Contrary to existing approaches, the proposed method utilizes short observation windows to identify inertia constants, thus presenting low computational complexity. This feature renders the proposed method suitable for real-time applications. Additionally, it is worth noting that the computational performance of the developed method is practically not affected by user-defined parameters, such as the order of the developed transfer function models.
- *Robustness*. A fully automated procedure is developed for the identification of unrealistic inertia estimates that may arise due to data quality issues. Therefore, the accuracy of the proposed method is not significantly affected by exogenous factors, such as the level of noise contained in measured responses.
- *Enhanced Accuracy*. The proposed method presents increased accuracy compared to existing conventional approaches.
- *Generic Applicability*. The proposed method can be used to identify inertia constants of: i) conventional SGs, ii) converter interfaced RESs, operated as virtual SGs (VSGs), and iii) virtual power plants (VPPs), hosting VSGs and constant power loads.

The rest of the paper is organized as follows: In Section II the theoretical background, required for the understanding of the proposed method, is provided. Algorithmic details for the implementation of the method are presented in Section III. In Section IV, the performance of the developed method is evaluated by performing RMS simulations on the IEEE 9-Bus Test System. Moreover, the impact of several factors, such as the noise level and the length of the analysis window, on the accuracy and the computational performance of the proposed method is assessed by means of Monte Carlo (MC) simulations. The application of the proposed method in the IEEE 39-Bus Test System is discussed in Section V. In Section VI comparisons with conventional techniques are presented. Finally, Section VII summarizes the main findings and concludes the paper.

II. Theoretical Background

A. The Swing Equation

Rotor dynamics of a SG can be modeled using the following form of the swing equation [12]:

$$2 \cdot H \cdot \frac{\mathrm{d}\Delta\omega(t)}{\mathrm{d}t} = \Delta_{p_m}(t) - \Delta_{p_e}(t) - D \cdot \Delta\omega(t). \quad (1)$$

Here, H and D denote the inertia constant and the damping coefficient of the machine, respectively. $\Delta\omega$ is the difference between the synchronous and the actual rotational speed. Δ_{p_m} and Δ_{p_e} stand for the change of the mechanical and electric power, respectively.

Eq. (1) can be further simplified to contain only variables measured on the electrical side. Indeed, immediately after a disturbance Δ_{p_m} can be considered equal to zero [12], [15]. Moreover, rotor speed deviation $\Delta\omega$ can be approximated using the frequency deviation at the connection bus of the machine, i.e., $\Delta\omega \approx \Delta f$ [12], [15]. Based on the above, (1) can be simplified to (2).

$$2 \cdot H \cdot \frac{\mathrm{d}\Delta f(t)}{\mathrm{d}t} = -\Delta_{p_e}(t) - D \cdot \Delta f(t). \quad (2)$$

The Laplace transform of (2) results in:

$$\frac{\Delta f(s)}{\Delta_{p_e}(s)} = -\frac{1/2H}{s + D/2H} \quad (3)$$

Here, $\Delta f(s)$ and $\Delta_{p_e}(s)$ are the bus frequency and the active power variation in the Laplace domain, respectively.

B. Inertia Estimation via Transfer Function Modelling

The unit impulse response $h(t)$ of (3) is given by (4), [14].

$$h(t) = -\frac{1}{2H} \cdot e^{-\frac{D}{2H} \cdot t} \quad (4)$$

Immediately after a disturbance, i.e., at $t = 0$, the value of the impulse response is determined only by the inertia constant H. Indeed, for $t = 0$, (4) gives:

$$h(0) = -\frac{1}{2H} \quad (5)$$

Based on the above analysis, it is clear that the inertia constant can be computed by applying a two-step procedure.

In the first step, a transfer function that describes the relationship between active power changes and frequency deviations shall be developed. The generic form of this transfer function is presented in (6).

$$G(s) = \frac{\Delta f(s)}{\Delta_{p_e}(s)} = \frac{\beta_{n-1}s^{n-1} + \beta_{n-2}s^{n-2} + ... + \beta_0}{\alpha_n s^n + \alpha_{n-1}s^{n-1} + ... + \alpha_0} \quad (6)$$

In the general case, the order n of $G(s)$ is higher compared to the order of (3), to allow for the accurate modeling of system dynamics. The required set of parameters, $\boldsymbol{\theta} = [\beta_{n-1}, \beta_{n-2}, ..., \beta_0, \alpha_n, \alpha_{n-1}, ..., \alpha_0]$, is identified by applying system identification techniques, such as the ARMAX method, the subspace state-space system identification (N4SID) technique, and the prediction error method (PEM).

In the second step, the impulse response of the identified transfer function is computed. As already discussed, $G(s)$ is more complex than the transfer function of (3). Nevertheless, even in this case, the inertial response is once again the fastest acting dynamic phenomenon that practically determines the first instance (value) of the impulse response [14]. Therefore, the inertia constant can be estimated by the value of the impulse response of $G(s)$ at $t = 0$. In particular, inertia constant can be computed as:

$$H_{est} = -\frac{1}{2 \cdot g(0)} \quad (7)$$

Here, g denotes the time domain impulse response of $G(s)$.

III. Proposed Method

In this paper, a new method for the on-line tracking of inertia constants is developed based on the SW concept. Each SW contains ambient responses of active power changes and frequency deviations, recorded at the terminals of generation devices. The length of each SW (t_w) is restricted to few seconds to ensure low computational complexity. The data refresh rate is equal to Δt_{rr}.

For each SW, an identification procedure is initially applied and a low-order input-output transfer function model is developed, describing the relationship between active power changes and frequency fluctuations. The inertia constant of the examined device is determined on a second stage, by computing the impulse response of the identified transfer function. The quality of the derived estimate is assessed using three validation criteria, described in detail in Section III-B. Nevertheless, it is worth noting that during the identification process erroneous estimates may occur, due to data quality issues. Therefore, in order to minimize the impact of erroneous estimates, the following procedure is proposed: Values of inertia constants, identified from several consecutive SWs, are collected to a database. This database is updated every Δt_{rr}. A statistical analysis of the observations, contained in the database, is performed in order to remove outliers, i.e., individual inertia estimates that differ significantly from all other observations. Outliers are removed using the interquartile range (IQR) rule [19]. The inertia constant of the examined generation device is finally defined as the mean value of the remaining observations, i.e., those not identified as outliers.

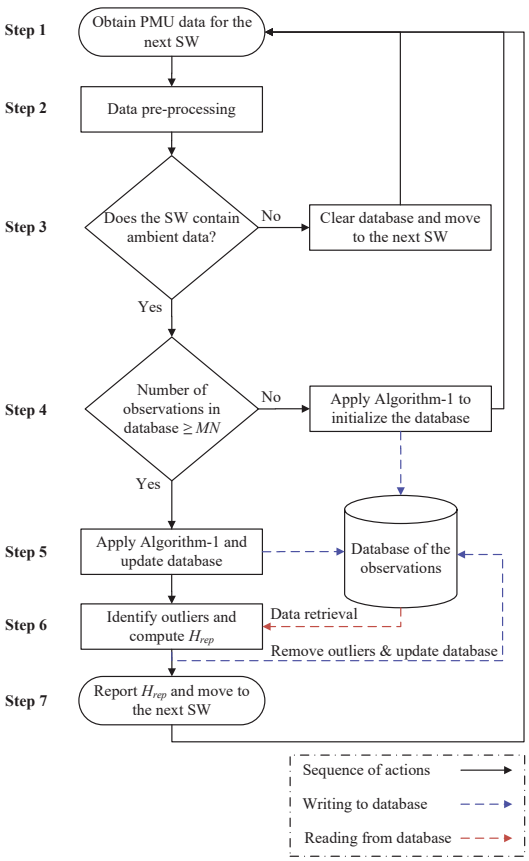

Fig. 1. Proposed method for the on-line tracking of inertia constants.

To apply the statistical analysis, a minimum number of observations (MN) must be available on the database. This minimum number of observations is obtained via an initialization phase. During the initialization, no results are reported to the system operator. The value of MN, and thus the duration of the initialization phase, is a user-defined parameter.

A. Implementation Details

The proposed method is presented in Fig. 1. A detailed analysis of all required steps is presented below:

Step-1: Phasor measurement unit (PMU) recordings for the examined SW are forwarded as inputs to the proposed method. The recordings contain ambient responses of frequency deviations and active power changes, obtained at the terminals of generation devices. The number of samples per second (sps) and the refresh rate, Δt_{rr}, of the SWs are determined by the system operator, based on the capabilities of the existing recording infrastructure. The length of the SW is set to t_w.

Step-2: A pre-processing of the recorded responses is performed. In particular, frequency and active power responses are converted to p.u. values and detrended.

Step-3: Inertia constants of VSGs and VPPs could be altered at any time for several reasons, e.g., reception of new dispatch signals, disconnection of RESs, etc. In such cases, inertia constants, derived by the proposed identification procedure (see Algorithm-1 of Section III-B), may be classified as outliers by the statistical analysis of Step-6, thus hindering accurate tracking/monitoring. To overcome this issue, the database of

inertia estimates shall be re-initialized every time the RoCoF and/or the rate of change of active power deviate significantly, compared to past values, i.e., every time a ringdown event occurs. The ringdown event can be triggered either by the change of individual inertia constants or by topological changes. Thus, in this Step, the proposed method checks if the examined SW contains only ambient data. If this is the case, the method proceeds to Step-4. Otherwise, the database is cleared and the method moves back to Step-1, i.e. to the next SW.

Step-4: The method checks if the number of observations contained in the database is adequate for statistical analysis, i.e., if the number of available observations is higher than MN. If this is the case, the method moves to the subsequent steps and reports the identified inertia constant to the user. Otherwise, the database shall be initialized. For this purpose, the identification procedure of Algorithm-1 is executed and the identified inertia constant is stored at the database. Subsequently, the method moves back to Step-1, i.e. to the next SW, without reporting the identified value to the system operator.

Step-5: Algorithm-1 is applied to the examined SW. The identified inertia constant is used to update the database.

Step-6: Initially, all observations are retrieved from the database and a statistical analysis is performed to determine outliers, i.e., individual estimates that differ significantly from all other observations contained in the database. To define outliers, the IQR is used [19]. In particular, the 25th percentile ($Q1$) and the 75th percentile ($Q3$) of the data contained in database are initially computed. Afterwards, IQR is calculated using (8). Observations with values lower than $Q1 - 1.5IQR$ or higher than $Q3 + 1.5IQR$ are classified as outliers and discarded. H_{rep} is defined as the mean value of the remaining observations, i.e., those not classified as outliers. Finally, the database is updated by removing all outliers.

$$IQR = Q3 - Q1 \tag{8}$$

Step-7: H_{rep} is reported to the system operator and the method moves to the next SW.

B. Identification Procedure

The identification procedure, applied to each SW to identify inertia constants, is presented in Algorithm-1, by means of pseudo-code. Algorithmic steps are explained in detail below:

Step-1: For each SW, a low-order transfer function model, $G(s)$, of the general form of (6), is developed to describe the input-output relationship between active power changes and frequency deviations. To ensure reduced computational complexity, the order n of the $G(s)$ is pre-defined by the user and remains constant throughout the analysis.

Step-2: Parameters of $G(s)$ are computed using ARMAX modeling. Further details concerning the parameter estimation procedure can be found in [11] and [16].

Step-3: The quality of the identified model is evaluated by means of fitting accuracy, i.e., by comparing the output of the identified transfer function with the actual recorded data. For this purpose, the error index (EI) of (9) is used.

$$EI = \left(1 - \frac{|x - y|}{|x - mean(x)|}\right) \cdot 100\%. \tag{9}$$

Algorithm 1 Identification procedure

1: Determine approximation order n, i.e., the order of $G(s)$ defined in (6).
2: Estimate parameters of $G(s)$ using ARMAX modeling.
3: Calculate the error index (EI) of (9).
4: Compute the impulse response of $G(s)$.
5: Use (7) to estimate inertia constant (H_{est}).
6: Perform a sanity check to evaluate the quality of the estimate.
7: **if** Sanity check is successful **then**
8: Forward the value of the computed H_{est} to the database.
9: **else**
10: Identification failed. No inertia estimate can be provided for this specific SW.
11: **end if**

Here, x denotes the recorded data and y the corresponding estimate. EI equal to 100% denotes a perfect approximation.

Step-4: The impulse response of the identified transfer function is computed.

Step-5: Eq. (7) is used to compute H_{est}.

Step-6: A sanity check is performed to evaluate the quality of the estimate. Towards this objective, three discrete validation criteria are considered. The first criterion is related to the stability of the identified transfer function. Indeed, only estimates derived from stable transfer functions are used for further analysis. The stability of the transfer function is assessed by computing its poles. The second validation criterion is related with the quality of the identified transfer function model. In general, the better the quality of the approximation is, the more accurate the inertia estimate [15]. Therefore, only estimates, resulted from models that present EI higher than a user-defined value/tolerance, are used. In this paper, EI tolerance is set to 80%. Finally, the value of the derived estimate shall be in a realistic range. Indeed, typical values for the inertia constants of SGs lie in the range between 2 s and 10 s [11], [20]. In this paper, a wider range is considered to also take into account VSGs. In particular, realistic H_{est} values are considered those that lie in the range (0 s, 15 s].

Step-7 to Step-11: A check is performed to verify that all validation criteria are met, i.e., the identified transfer function is stable, $EI \geq 80\%$, and $H_{est} \in (0\text{ s}, 15\text{ s}]$. If the check is successful, then the derived estimate is forwarded to the database. Otherwise, no action is performed, i.e., the identification procedure failed to provide a reliable estimate, and thus the process shall continue with the next SW.

IV. Validation of the Proposed Method On the IEEE 9-Bus Test System

In this Section, MC simulations are preformed to quantify the impact of several factors on the performance of the proposed method. In particular, the impact of: i) the approximation order, ii) the length of the analysis window, iii) the refresh rate of the data, and iv) the noise level, on the accuracy and the computational performance of the proposed method is investigated.

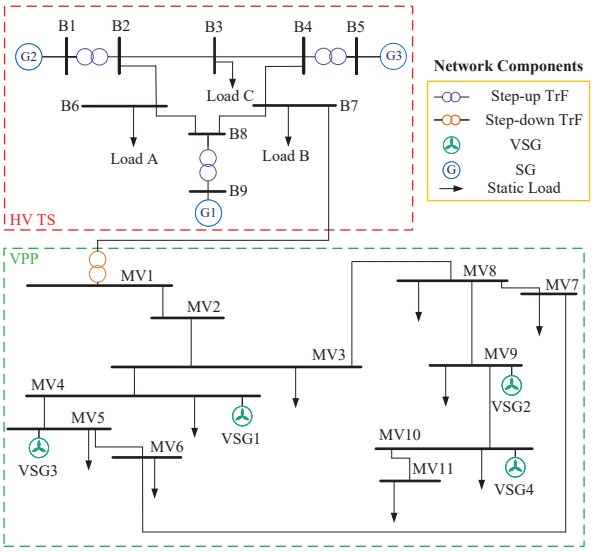

Fig. 2. Topology of the IEEE 9-Bus Test System and the examined VPP.

A. System Under Study

The performance of the proposed method is evaluated by means of RMS simulations performed on the DIgSILENT software [21], using the power system depicted in Fig. 2. The examined system consists of a high voltage TS and a VPP.

The TS is a modified version of the IEEE 9-Bus Test System [22] and contains 3 conventional SGs. Their inertia constants are $H_{G1} = 2.63$ s, $H_{G2} = 4.13$ s, $H_{G3} = 4.77$ s. The VPP is based on the topology of the European benchmark medium-voltage grid of CIGRE [23] and it is comprised by 9 constant power loads and 4 RESs, operated as VSGs. Details concerning the modeling of the VSGs can be found in [6]. The rated power of all RESs is equal to 1 MVA. The inertia constants of the VSGs are: $H_{VG1} = 4$ s, $H_{VG2} = 5$ s, $H_{VG3} = 6$ s, $H_{VG4} = 8$ s. The equivalent inertia constant of the VPP is computed as:

$$H_{VPP}^{eq} = \frac{\sum_{k=1}^{4} H_{VG,k} \cdot S_{VG,k}}{\sum_{k=1}^{4} S_{VG,k}} = 5.75 \text{ s}. \qquad (10)$$

In (10), $H_{VG,k}$ and $S_{VG,k}$ are the inertia constant and the rated power of the k-th VSG, respectively.

B. On-line Tracking of Inertia Constants

Initially, the proposed method is used to identify under ambient conditions the inertia constants of SGs, VSGs, and VPPs. Ambient responses are generated for 65 s, by applying small random variations to the power consumption of all loads connected to the TS, i.e., loads A, B, and C of Fig. 2. The applied power variations are lower than 2% of the rated power of the loads, thus ensuring small frequency fluctuations, imitating ambient (normal) operating conditions. Indicative frequency responses, as recorded at the connection buses of G1, G2, and G3, are plotted in Fig. 3.

For all the installed SGs and VSGs, frequency deviations and active power variations at the point of interconnection (POI) with the utility grid are recorded. Frequency and active power fluctuations are also recorded at the point of common coupling (PCC) of the VPP with the TS (PCC is located at Bus MV1 of Fig. 2). All responses are acquired with a sampling rate of 100 sps. Responses, recorded from each generation device, are forwarded as inputs to the proposed method and the corresponding inertia constants are identified. For the identification the following settings are used: $n = 2$, $\Delta t_{rr} = 0.5$ s, $t_w = 5$ s, $MN = 5$.

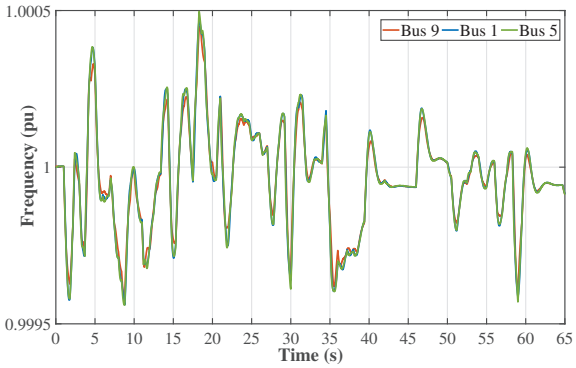

Fig. 3. Frequencies of buses B1, B5, and B9 of the system of Fig. 2.

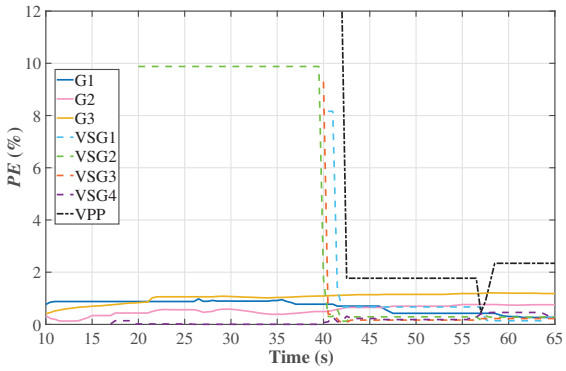

Fig. 4. IEEE 9-Bust Test System. Evolution of PE with respect to time.

To quantify the accuracy of the estimates, the following prediction error, PE, is introduced:

$$PE(\%) = \frac{|H_{true} - H_{rep}|}{H_{true}} \cdot 100\% \qquad (11)$$

Here, H_{true} is the actual inertia of the examined device; H_{rep} is the inertia constant reported by the proposed method.

The time evolution of PE, for all examined devices, is presented in Fig. 4. As shown, for each one of the examined devices, the proposed method starts providing inertia estimates at different time moments. For instance, for G1, G2, and G3 inertia estimates are provided 10 s after the triggering of the method; For VSG4 and VSG2 after 17 s and 20 s, respectively. Finally, for VSG1, VSG3 and for the VPP the inertia estimates are provided 40 s after the triggering of the method. In fact, this is the time required for the initialization of each one of the corresponding databases, i.e., the time needed to obtain the initial *MN* observations that are required for the statistical analysis applied at Step-6 of the proposed method (Step-6 of Fig. 1). Once the databases are initialized, the proposed method converges very fast to the actual inertia constant, resulting, for all examined devices, in PE lower than 2.5%.

TABLE I
IMPACT OF APPROXIMATION ORDER ON PE (%).

	n = 2	n = 3	n = 4	n = 5	n = 6
μ	0.60	1.45	1.55	1.68	1.71
std	0.34	1.23	1.21	1.16	1.12

TABLE II
IMPACT OF WINDOW LENGTH ON PE (%).

	t_w = 2.5 s		t_w = 5 s		t_w = 10 s	
Order	μ	std	μ	std	μ	std
n = 2	0.62	0.36	0.60	0.34	0.80	0.61
n = 3	1.60	1.36	1.45	1.23	1.67	0.98
n = 4	1.60	1.55	1.55	1.21	1.73	2.10
n = 5	1.62	1.75	1.68	1.16	1.68	1.01
n = 6	1.70	2.03	1.71	1.12	1.56	0.97

C. Impact of Approximation Order

The impact of the approximation order on the accuracy of the proposed method is quantified by means of MC analysis. In particular, 100 discrete MC simulations are performed as follows: For each MC, 65 s of ambient data are generated by applying small variations to the power consumption of TS loads. During each simulation, more than 100 power variations are imposed. To ensure normal operation conditions, the maximum applied power variation is lower than 2% of the rated power of the loads. During the 65 s of each simulation, the grid frequency remains between 49.9 Hz and 50.1 Hz.

For each MC simulation, frequency and active power variations of all installed SGs are acquired at a sampling rate of 100 sps. These responses are forwarded as inputs to the proposed method and inertia constants are identified using the following settings: $\Delta t_{rr} = 0.5$ s, $t_w = 5$ s, $MN = 5$, $n = 2$. The approximation order, n, ranges from 2 up to 6.

The mean (μ) and the standard deviation (std) of the resulting PE across the 100 MC, for all examined approximation orders, are summarized in Table I. Results reveal that the performance of the proposed method is practically unaffected by the approximation order. Indeed, in all cases, the mean value for the PE is lower than 2%.

D. Impact of window length

The impact of window length on the accuracy of the proposed method is quantified using the ambient responses generated during the MC analysis of Section IV-C. However, here, three discrete cases are considered for t_w, namely $t_w = 2.5$ s, $t_w = 5$ s, and $t_w = 10$ s. In all cases, n varies from 2 up to 6, while $\Delta t_{rr} = 0.5$ s and $MN = 5$.

Results across the 100 MC for all examined cases are summarized in Table II. As shown, in all combinations of model orders and window lengths the mean value of the PE is lower than 2%, verifying the accuracy of the method.

E. Impact of refresh rate

Ambient responses, generated at Section IV-C, are also used to evaluate the influence of refresh rate on the accuracy of the proposed method. For the identification of inertia constants, the following settings are used: $t_w = 5$ s, $MN = 5$, n varies from 2 up to 6. Three refresh rates are tested, i.e., Δt_{rr} can be 0.25 s, 0.5 s, or 1 s. Results across the 100 MC simulations are reported in Table III. It is evident that the impact of refresh rate on the accuracy of the proposed method is rather trivial.

TABLE III
IMPACT OF REFRESH RATE ON PE (%).

	Δt_{rr} = 0.25 s		Δt_{rr} = 0.5 s		Δt_{rr} = 1 s	
Order	μ	std	μ	std	μ	std
n = 2	0.60	0.33	0.60	0.34	0.61	0.37
n = 3	1.43	1.19	1.45	1.23	1.60	1.19
n = 4	1.54	1.19	1.55	1.21	1.61	1.22
n = 5	1.62	1.15	1.68	1.16	1.62	1.15
n = 6	1.62	1.10	1.71	1.12	1.60	1.16

F. Impact of noise

The impact of noise on the performance of the proposed method is evaluated by distorting the simulated ambient responses with additive white Gaussian noise (AWGN). The variance of the AWGN is adjusted to replicate two levels of signal-to-noise (SNR) ratios. The examined SNR levels are 45 dB and 30 dB. For each SNR level, 100 MC simulations are performed, representing discrete instances of noise. For each MC simulation, ambient responses of all installed SGs are used to identify the corresponding inertia constants. For the identification procedure, the following settings are used $\Delta t_{rr} = 0.5$ s, $t_w = 5$ s, $MN = 5$, $n = 2$.

Indicative results are presented in Fig. 5 by means of boxplots. The boxplots contain estimates resulted from all SWs that were examined across the 100 MCs. As shown, for both SNR levels the median value of the PE is well below 5%, verifying the accuracy of the method under noisy conditions.

G. Computational performance

The computational performance of the proposed method is quantified by analyzing the required execution time, i.e., the time needed for the completion of Algorithm-1 and the updating of the database. Several scenarios are examined, assuming discrete window lengths and approximation orders.

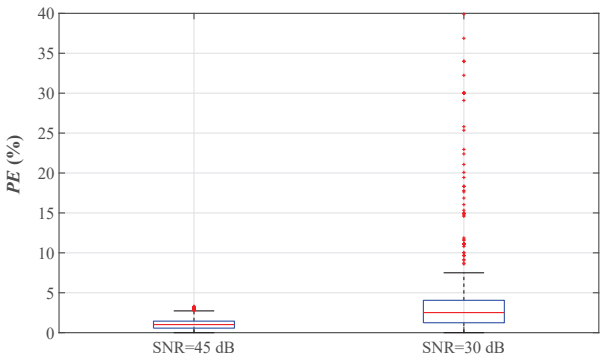

Fig. 5. Performance of the proposed method under noisy conditions.

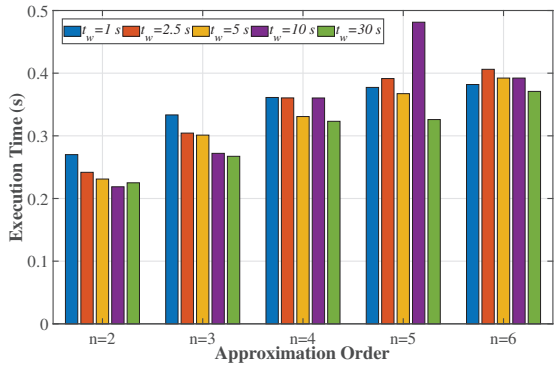

Fig. 6. Computational performance of the proposed method.

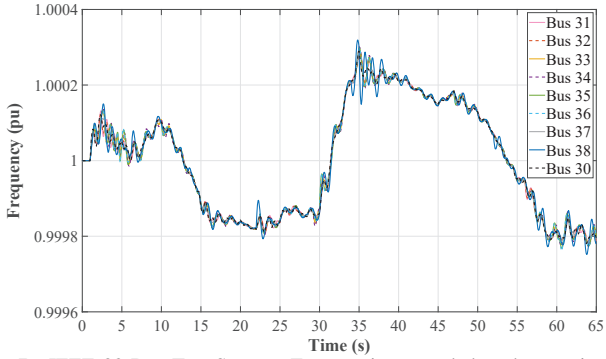

Fig. 7. IEEE 39-Bus Test System. Frequencies recorded at the terminals of SGs.

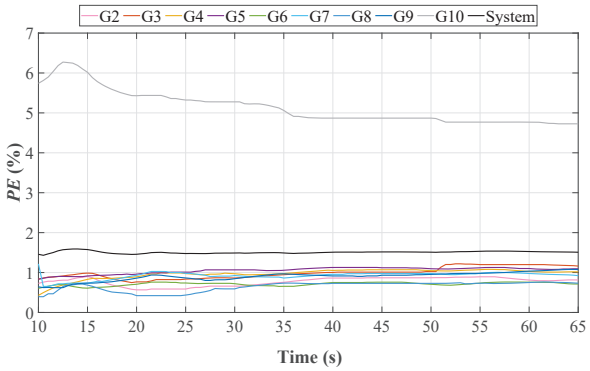

Fig. 8. IEEE 39-Bus Test System. Evolution of PE with respect to time.

Concerning the length of the analysis window, five cases are considered, namely $t_w = 1$ s, $t_w = 2.5$ s, $t_w = 5$ s, $t_w = 10$ s, and $t_w = 30$ s. Regarding the approximation order, the following cases are examined: $n = 2$, $n = 3$, $n = 4$, $n = 5$, and $n = 6$. For each combination of t_w and n a set of 100 MC simulations is performed using an i7-8750H, 2.2 GHz, 12 GB RAM personal computer. For each set of MC simulations, the resulting mean execution time is computed and reported in Fig. 6. As shown, as n increases, the average execution time increases as well. Nevertheless, in all cases, the average execution time is lower than 0.5 s. This low computational burden renders the proposed method appropriate for close-to-real-time monitoring applications.

H. Discussion of the Results

The presented analysis reveals that the proposed method performs satisfactorily under noisy conditions. Additionally, the results of Sections IV-C, IV-D, and IV-E, indicate that the approximation order (n), the length of the SW (t_w), and the refresh rate of the data (Δt_{rr}) do not affect considerably the accuracy of the method. This is an important remark, since all the above-mentioned parameters are user-defined. Moreover, it is worth noting that in all examined cases the mean execution time of the proposed method is lower than 0.5 s.

Based on the presented analysis, the following settings are suggested for the implementation of the proposed method: $n = 2$, $t_w = 5$ s, and $\Delta t_{rr} = 0.5$ s. Indeed, the most accurate estimates are derived when $n = 2$. Theoretically, a first-order transfer function should be sufficient, since the swing equation is described by (3). Nevertheless, as discussed in [14]–[16], higher order models are generally required to account the impact of additional system dynamics such as the intra-area and inter-area oscillations. t_w is set to 5 seconds to ensure that only the most recent data are used for the identification of inertia constants. Additionally, for $t_w = 5$ s the execution time is always lower than 0.5 s. Thus, a refresh rate of 0.5 s, i.e., $\Delta t_{rr} = 0.5$ s, is sufficient for the application of the method.

V. Application of the Proposed Method in the IEEE 39-Bus Test System

The proposed method is also tested on the IEEE 39-bus Test System [22]. The examined system is simulated in DIgSILENT and consists of 10 generators, 19 loads, 39 buses, 12 transformers, and 34 lines. Generator 1 is an equivalent generator that is used to represent the external power grid. All other generators, i.e., G2 up to G10, belong to the internal (the examined) power system and they are equipped with automatic voltage regulators and governors. Ambient data are generated for 65 s by applying small random variations to the power consumption of all system loads. The frequency responses at the connection buses of G2-G10 are reported in Fig. 7.

The proposed method is used to identify inertia constants of all SGs of the examined system. Additionally, the overall power system inertia is computed (using Eq. (8) of [11]) and compared with the estimate provided by the proposed method. The resulting PE with respect to time is depicted in Fig. 8. As shown, for all examined SGs as well as for the overall inertia constant, i.e., the system inertia, the corresponding PE converge to values lower than 5%, verifying the accuracy of the proposed method.

VI. Comparisons with Conventional Techniques

Here, the proposed method is compared against the method of [13]. Similar to the proposed method, the approach of [13] uses the SW concept to identify inertia constants from ambient data. Nevertheless, the approach of [13] presents fundamental differences compared to the proposed method.

In particular, the method of [13] uses the N4SID technique to identify the parameters of the required transfer functions. The optimal order of the transfer functions is defined through a grid search approach. In fact, transfer function models with orders varying from 1 up to 10 are tested. The model that

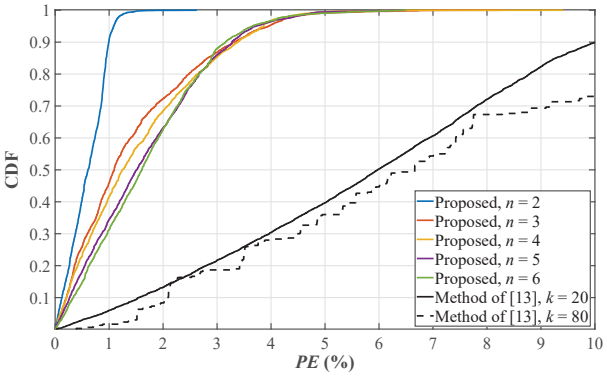

Fig. 9. CDFs of the PE for the proposed method (assuming discrete model orders) and the method of [13].

results in the maximum fitting accuracy is used for inertia estimation. Inertia estimates are derived for each SW by computing the initial slope of the unit step response of the identified transfer functions [18]. Finally, inertia constants, reported to the system operator, are computed using (12).

$$H_t = \begin{cases} \xi_t^k \cdot h_t + (1 - \xi_t^k) \cdot H_{t-1}, & \text{if stable,} \\ H_{t-1}, & \text{if unstable} \end{cases} \tag{12}$$

Where, H_t and H_{t-1} are the inertia constants reported during the current and the previous SW, respectively. h_t is the inertia constant identified using measurements obtained only from the current SW. ξ_t is a fitting coefficient, computed at the current SW. In this paper, ξ_t is equal to EI divided by 100. k is an exponent used to smooth the impact of low quality estimates on the final reported inertia constant value. According to [13], k can vary between 20 and 80. For the comparisons, two cases are considered, i.e., $k = 20$ and $k = 80$.

Comparisons are performed using the ambient responses of Section IV-C. Results are summarized in Fig. 9 by means of cumulative distribution functions (CDFs). More specifically, the CDFs are composed using the PE resulted from all SWs that were examined across the 100 MC simulations. For the proposed method, $\Delta t_{rr} = 0.5$ s, $t_w = 5$ s, and $MN = 5$, while n varies from 2 up to 6. For each discrete approximation order, a dedicated CDF is computed. As shown in Fig. 9 in all cases the proposed method presents superior performance compared to the conventional approach of [13].

VII. Conclusions and Future Work

In this paper, a new method is proposed for the identification of inertia constants from ambient responses. The proposed method is tested by means of simulations on two benchmark power system models, namely the IEEE 9-Bus Test System and the IEEE 39-Bus Test System. The impact of several factors, such as the noise level, the length of the analysis window, and the approximation order, is thoroughly tested by means of MC simulations. Analysis reveals that the proposed method can accurately estimate inertia constants of SGs, VSGs, and VPPs, while presenting low computational complexity.

The proposed method can be used by system operators for the development of on-line applications that aim to quantify the contribution of different generation devices to the provision of inertial response. These applications will ensure the fair remuneration of all participants in inertia AS markets. Further research will be performed to develop new methods, aiming to quantify the effective inertia of active distribution networks that host: frequency-dependent loads, storage systems equipped with fast frequency response functionalities, and RESs that provide virtual inertia.

References

[1] G. C. Kryonidis, *et. al*, "Ancillary services in active distribution networks: A review of technological trends from operational and online analysis perspective," *Renew. Sust. Energ. Rev.*, vol. 147, 2021.

[2] H. Bevrani, H. Golpira, A. R. Messina, N. Hatziargyriou, F. Milano, and T. Ise, "Power system frequnecy control: An updated review of current solutions and new challenges," *Electr. Power Syst. Res.*, vol. 194, 2021.

[3] ENTSO-E, "High penetration of power electronic interfaced power sources and the potential contribution of grid forming converters," Technical Report, 2019.

[4] CIGRE, "Impact of high penetration of inverter-based generation on system inertia of networks," Technical Report, 2021.

[5] U. Tamrakar, D. Shrestha, M. Maharjan, B. P. Bhattarai, T. M. Hansen, and R. Tonkoski, "Virtual inertia: Current trends and future directions," *Appl. Sci.*, vol. 7, no. 7, 2017.

[6] G. C. Kryonidis, K. N. D. Malamaki, J. M. Mauricio, and C. S. Demoulias, "A new perspective on the synchronverter model," *Int. J. Electr. Power Energy Syst.*, vol. 140, 2022.

[7] K. O. Oureilidis, *et. al*, "Ancillary services market design in distribution networks: Review and identification of barriers," *Energies*, vol. 13, 2020.

[8] A. Rodriguez del Nozal, E. O. Kontis, J. M. Mauricio, and C. S. Demoulias, "Provision of inertial response as ancillary service from active distribution networks to the transmission system," *IET Gener. Transm. Distrib.*, vol. 14, no. 22, pp. 5123–5134, 2020.

[9] ENTSO-E, "Future system inertia 2," Technical Report, 2018.

[10] B. Tan, J. Zhao, M. Netto, V. Krishnan, V. Terzija, and Y. Zhang, "Power system inertia estimation: Review of methods and the impacts of converter-interfaced generations," *Int. J. Electr. Power Energy Syst.*, vol. 134, 2022.

[11] S. C. Dimoulias, E. O. Kontis, and G. K. Papagiannis, "Inertia estimation of synchronous devices: Review of available techniques and comparative assessment of conventional measurement-based approaches," *Energies*, vol. 15, no. 20, 2022.

[12] J. Zhang and H. Xu, "Online identification of power system equivalent inertia constant," *IEEE Trans. Ind. Electron.*, vol. 64, no. 10, pp. 8098–8107, 2017.

[13] F. Zeng, J. Zhang, G. Chen, Z. Wu, S. Huang, and Y. Liang, "Online estimation of power system inertia constant under normal operating conditions," *IEEE Access*, vol. 8, pp. 101 426–101 436, 2020.

[14] K. Tuttelberg, J. Kilter, D. Wilson, and K. Uhlen, "Estimation of power system inertia from ambient wide area measurements," *IEEE Trans. Power Syst.*, vol. 33, no. 6, pp. 7249–7257, 2018.

[15] L. Lugnani, D. Dotta, C. Lackner, and L. Chow, "c," *Electr. Power Syst. Res.*, vol. 180, 2020.

[16] E. Kontis, I. Pasiopoulou, D. Kirykos, T. Papadopoulos, and G. Papagiannis, "Estimation of power system inertia: A comparative assessment of measurement-based techniques," *Electr. Power Syst. Res.*, vol. 196, 2021.

[17] D. Yang, G. Cai, J. Ma, J. Tian, Z. Chen, and L. Wang, "Inertia-adaptive model predictive control-based load frequency control for interconnected power systems with wind power," *IET Gener. Transm. Distrib.*, vol. 14, no. 22, pp. 5029–5036, 2020.

[18] F. Zeng, J. Zhang, Y. Zhou, and S. Qu, "Online identification of inertia distribution in normal operating power system," *IEEE Trans. Power Syst.*, vol. 35, no. 4, pp. 3301–3304, 2020.

[19] F. M. Dekking, C. Kraaikamp, H. P. Lopuhaä, and L. E. Meester, *A Modern Introduction to Probability and Statistics*. London: Springer, 2006.

[20] P. Tielens and D. V. Hertem, "The relevance of inertia in power systems," *Renewable and Sustainable Energy Reviews*, vol. 55, 2016.

[21] DIgSILENT GmbH, DIgSILENT Solutions PowerFactory Version 20.

[22] https://www2.kios.ucy.ac.cy/testsystems/.

[23] CIGRE, "Benchmark systems for network integration of renewable and distributed energy resources," *CIGRE Task Force C6.04.02*, 2014.